

Molecular probe to visualize the effect of a glycolytic inhibitor on reducing NADH levels in a cellular system

Pooja Dhingra, Kajal Jaswal, Bidisha Biswas, Iswar Chandra Mondal, Prosenjit Mondal,

Subrata Ghosh

Table of Contents:

S. No.	Contents	Page No.
1.	Experimental procedures and calculations	S2-S3
2.	Synthesis outline and procedure for the development of MQ-CN-BTZ	S3-S5
3.	Synthesis outline and procedure for the development of MQ-CN-BTZH	S6
4.	^1H -NMR, ^{13}C -NMR and Mass spectra	S7-S14
5.	Optical behaviour of MQ-CN-BTZ	S15-S17
6.	MTT assay for MQ-CN-BTZ	S18
7.	Table S3: Performance parameters of some of the reported efficient probes for NADH/NADPH detection and cellular imaging.	S18-S20
8.	References	S20-S22

1. Experimental procedures and calculations

Sample Preparation for Biomolecules Screening:

Different analytes such as amino acids, cations, anions, reactive sulfur species (RSS), reactive oxygen species (ROS), and other relevant species were added to the PBS buffer solution and sonicated for a short time for dissolving the analytes to get the stock solution. For various anions and cations, the tetrabutylammonium salts and nitrate salts were used, respectively.

Cell line and cell culture conditions:

For *in vitro* experiments Human hepatocellular carcinoma cell lines (HepG2) was used. Dulbecco's minimal essential media (DMEM) was used for maintaining the cell line and then, the cell line was supplemented with 10% FBS (fetal bovine serum) and 1% penicillin streptomycin (PenStrep) and the cells were maintained at 37 °C in 5% CO₂.

Treatment of the dye MQ-CN-BTZ:

10 mM stock solution of the dye was made by dissolving in HPLC grade DMSO. For the successive experiments, 5 μ M was used as the working concentration. While performing *in vitro* experiments, HepG2 cells were incubated with dye for two hours at 37 °C and DMSO was used as vehicle control.

In vitro experiments

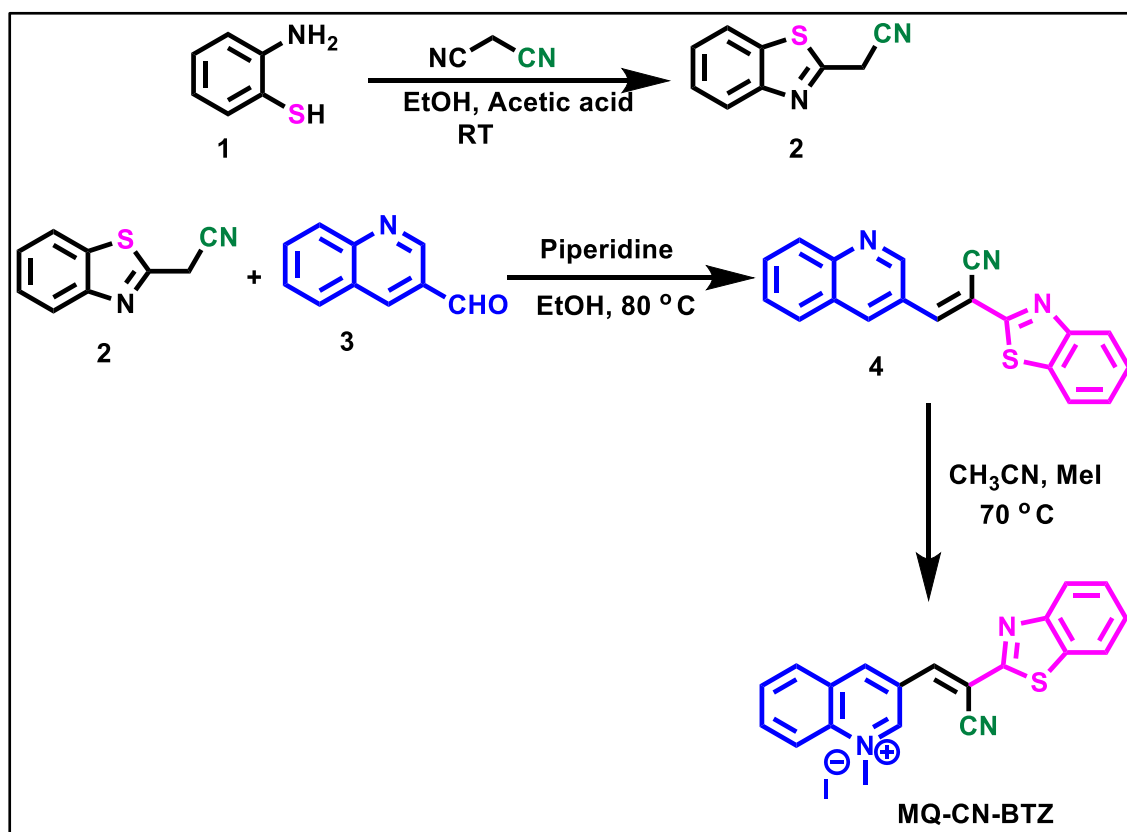
Cytotoxicity assay for the dye:

The MTT assay was performed to check the cytotoxicity of **MQ-CN-BTZ** in the cells. Firstly, 8000 cells were seeded in 96 well plate for 24 hours and then the cells were treated with different concentration of dye (0, 2.5, 5, 7.5, 10, 12.5 and 15 μ M) for 24 hours. After that, the cells were treated with MTT dye (0.5 mg/ml) for 4 hours. Media from cells was removed and the formed formazan crystals were dissolved in 200 μ L of DMSO. Using iMark plate reader (BIORAD), the absorbance at 570 nm was measured. The viability of the cells was expressed as percent cell viability relative to the control.

Inhibitor experiment protocol:

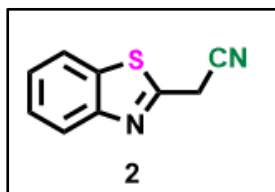
Firstly, the coverslips were coated with PLL (poly-L-lysine) and then, the HepG2 cells were seeded on the coverslips for 12 hours. After that, the cells were treated with 3-bromopyruvic acid inhibitor (50 and 150 μM) for half hour in serum free media. Then, the cells were incubated with 5 μM **MQ-CN-BTZ** for 2 hours in serum free media and further, the cells were incubated at 37°C. Post treatment the cells were washed with PBS three times for 5 mins each and then mounted onto glass slides using mounting agent as DAPI and then the imaging was done using confocal microscopy.

2. Synthesis outline and procedure for MQ-CN-BTZ



Scheme S1. Synthesis route for **MQ-CN-BTZ**

Synthesis of 2



Compound 2 has been synthesized following the reported literature method.¹⁻⁴

Spectroscopic details of 2:

¹H NMR (500 MHz, CDCl₃), δ (ppm): 8.05 (d, *J* = 8.1 Hz, 1H), 7.90 (d, *J* = 8.0 Hz, 1H), 7.55-7.52 (m, 1H), 7.47-7.44 (m, 1H), 4.25 (s, 2H).

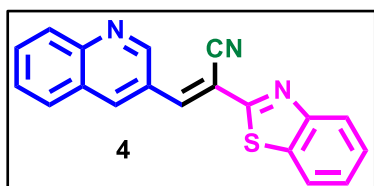
¹³C NMR (125 MHz, CDCl₃), δ (ppm): 158.2, 152.8, 135.4, 126.7, 125.9, 123.3, 121.7, 114.9, 23.2.

HRMS (ESI): Calc. for C₉H₅N₂S [M-H]⁻: 173.0173; Found: 173.0171.

Physical Properties: Yellow solid.

% Yield: ~ 36%

Synthesis of 4:



A solution of **2** (benzothiazol-2-yl acetonitrile) (1 equiv) and quinoline-3-carboxaldehyde (**3**) (1.07 equiv) in ethanol (5 mL) was stirred for 5 min at room temperature and then piperidine (one drop) was added to the solution, and the resulting mixture was heated at 80° C for 3 h. The reaction was monitored using thin layer chromatography. After completion of the reaction, the mixture was cooled down to room temperature and then, the yellow precipitate was filtered off and washed with cold ethanol for several times to afford **4** as yellow solid with ~ 80% yield.

Spectroscopic details of 4:

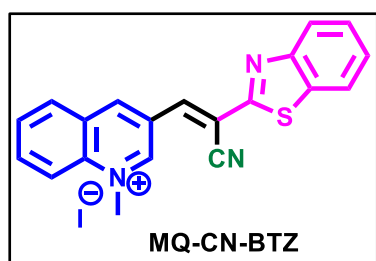
¹H NMR (500 MHz, CDCl₃), δ (ppm): δ 9.23 (d, *J* = 2.25 Hz, 1H), 9.09 (d, *J* = 2.15 Hz, 1H), 8.42 (s, 1H), 8.16-8.11 (m, 2H), 8.00-7.94 (m, 2H), 7.87-7.84 (m, 1H), 7.68-7.65 (m, 1H), 7.58-7.55 (m, 1H), 7.49-7.46 (m, 1H).

¹³C NMR (125 MHz, CDCl₃), δ (ppm): 161.9, 153.5, 151.5, 149.0, 142.8, 136.7, 135.1, 132.1, 129.4, 129.2, 127.9, 127.3, 127.2, 126.3, 125.5, 123.8, 121.8, 116.2, 107.4.

HRMS (ESI): Calc. for C₁₉H₁₂N₃S [M+H]⁺: 314.0752; Found: 314.0753

Physical Properties: Yellow solid.

Synthesis of MQ-CN-BTZ:



In a sealed tube, compound 4 (1 eq) was dissolved in acetonitrile (1 mL), and then methyl iodide (3 eq) was added dropwise and stirred at room temperature for 30 min. Then, the reaction mixture was heated at 70° C for 3 h. The progress of the reaction was monitored using thin layer chromatography. Then, the reaction mixture was cooled to room temperature. The orange precipitate was filtered off and washed with diethyl ether for 5 times to obtain **MQ-CN-BTZ** as orange solid with ~ 80% yield.

Spectroscopic details of compound MQ-CN-BTZ:

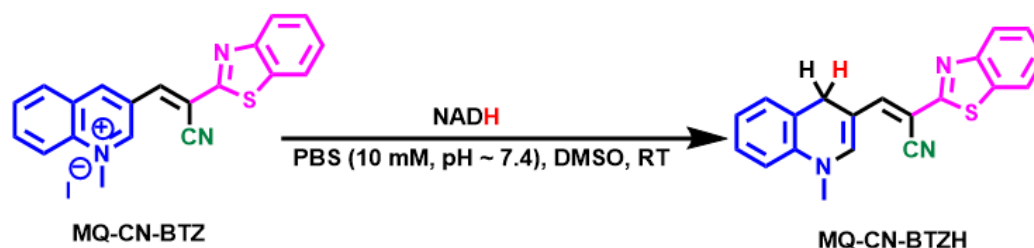
¹H NMR (500 MHz, DMSO-*d*₆), δ (ppm): 10.01 (s, 1H), 9.86 (s, 1H), 8.73 (s, 1H), 8.64-8.60 (m, 2H), 8.41 (t, *J* = 7.95 Hz, 1H), 8.30 (d, *J* = 7.95 Hz, 1H), 8.20-8.15 (m, 2H), 7.68-7.60 (m, 2H), 4.70 (s, 3H).

¹³C NMR (125 MHz, DMSO-*d*₆), δ (ppm): 161.6, 153.0, 151.5, 145.5, 141.2, 138.4, 137.3, 134.8, 131.5, 131.0, 128.7, 127.6, 127.1, 126.8, 123.7, 122.8, 119.6, 115.0, 111.3, 46.1.

HRMS (ESI): Calc. for C₂₀H₁₄N₃S [M-I]⁺: 328.0903; Found: 328.0901

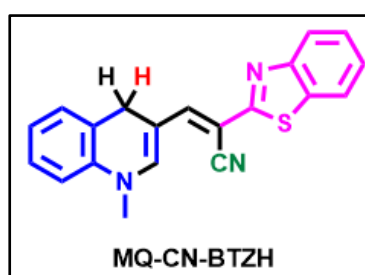
Physical Properties: Orange solid.

3. Synthesis outline and procedure for MQ-CN-BTZH



Scheme S2. Synthesis route for **MQ-CN-BTZH**.

Synthesis of MQ-CN-BTZH:



NADH (1.1 eq) was taken in a round bottom flask and dissolved in PBS buffer (~7.4 pH, 7 mL). A solution of **MQ-CN-BTZ** (1 eq) in DMSO (2 mL) was added to the solution of NADH and the resulting mixture was stirred at room temperature for 1 hour. The progress of the reaction was monitored using thin-layer chromatography. After completion, the reaction mixture was extracted with dichloromethane. The extracted organic layer was dried over sodium sulfate and concentrated using rotavapor. Further, the crude was purified using column chromatography (a mixture of ethyl acetate and hexane was used as eluent) to obtain **MQ-CN-BTZH** as a dark-orange solid with ~ 75% yield.

Spectroscopic details of MQ-CN-BTZH:

¹H NMR (500 MHz, CDCl₃), δ (ppm): 7.89 (d, *J* = 8.1 Hz, 1H), 7.79 (d, *J* = 7.9 Hz, 1H), 7.66 (s, 1H), 7.41 (t, *J* = 7.8 Hz, 1H), 7.28 (t, *J* = 7.8 Hz, 1H), 7.18-7.13 (m, 2H), 7.02 (t, *J* = 7.5 Hz, 1H), 6.81-6.79 (m, 2H), 4.37 (s, 2H), 3.31 (s, 3H).

¹³C NMR (125 MHz, CDCl₃), δ (ppm): 166.0, 153.9, 148.1, 146.9, 137.3, 134.4, 130.2, 127.5, 126.3, 124.7, 124.3, 123.3, 122.1, 121.4, 119.5, 113.5, 107.7, 91.9, 39.6, 26.9.

HRMS (ESI): Calc. for C₂₀H₁₆N₃S [M+H]⁺: 330.1065; Found: 330.1061

Physical Properties: Dark orange solid.

4. ^1H -NMR, ^{13}C -NMR and Mass spectra

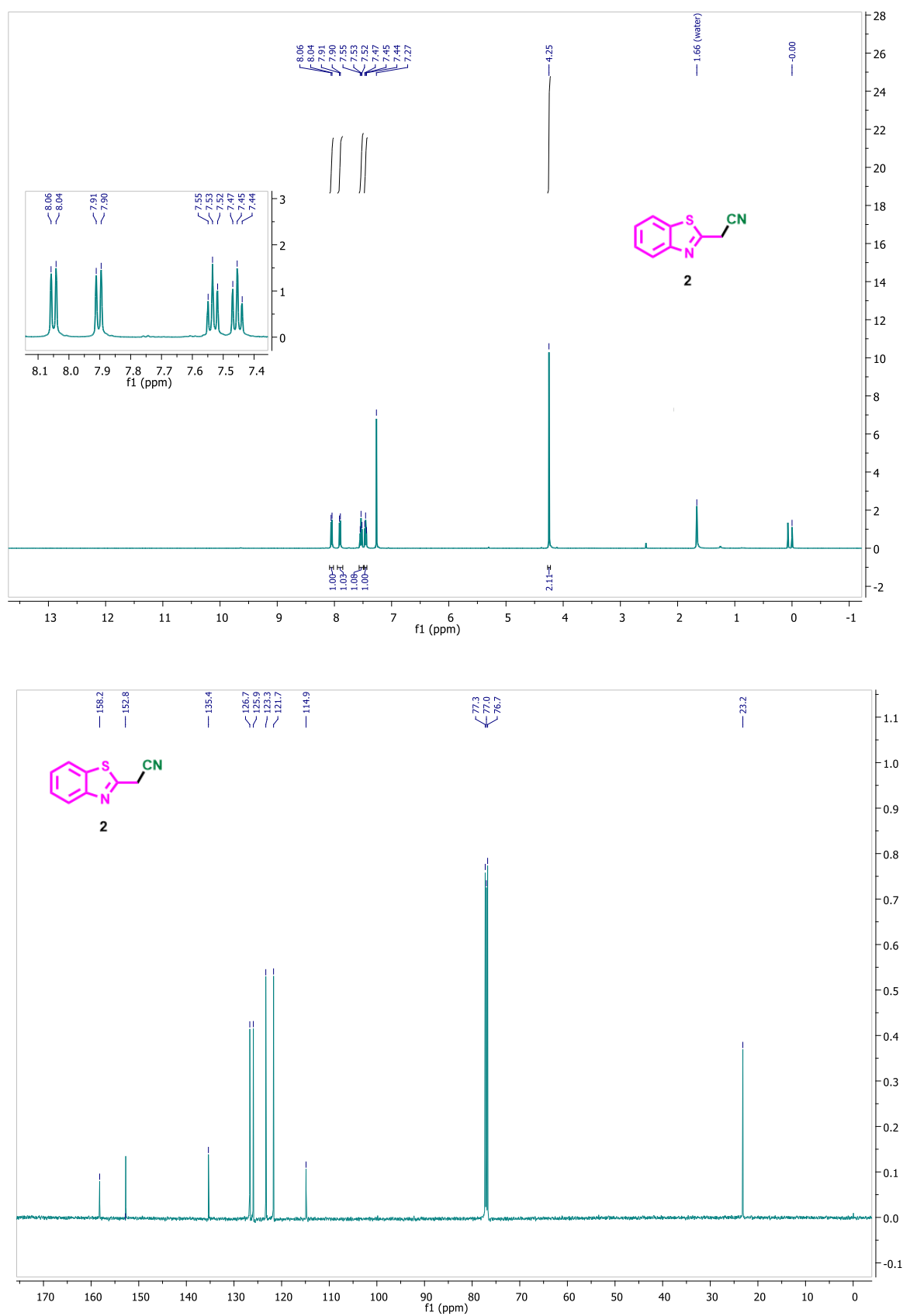


Figure S1. ^1H and ^{13}C NMR spectra of compound **2**

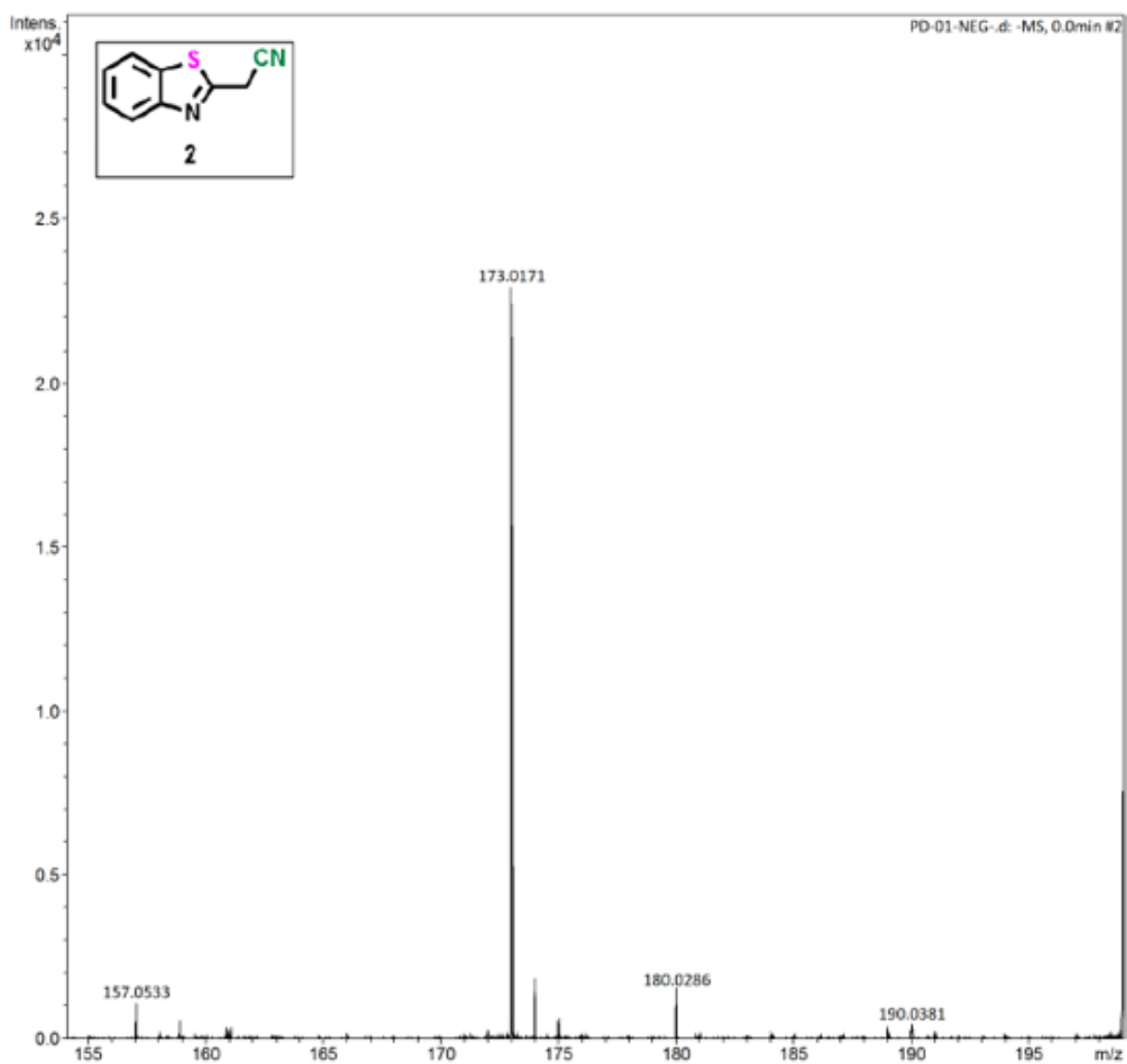
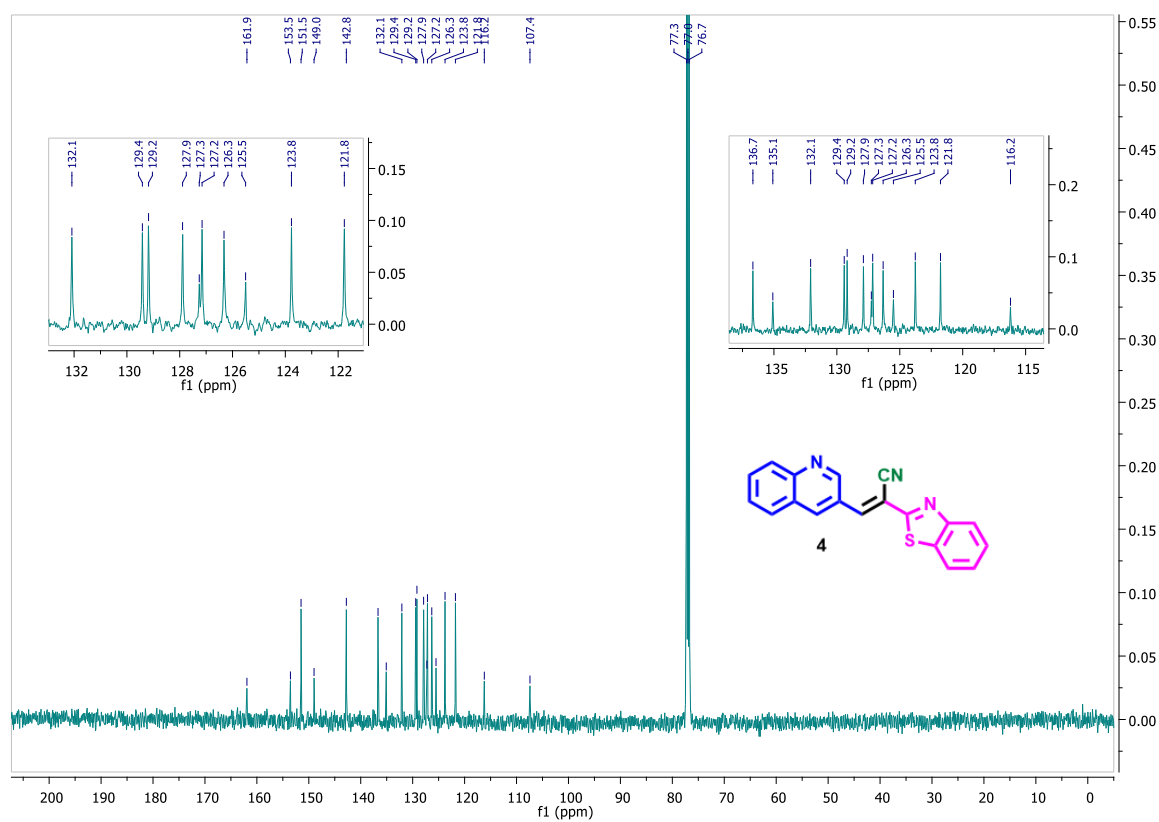
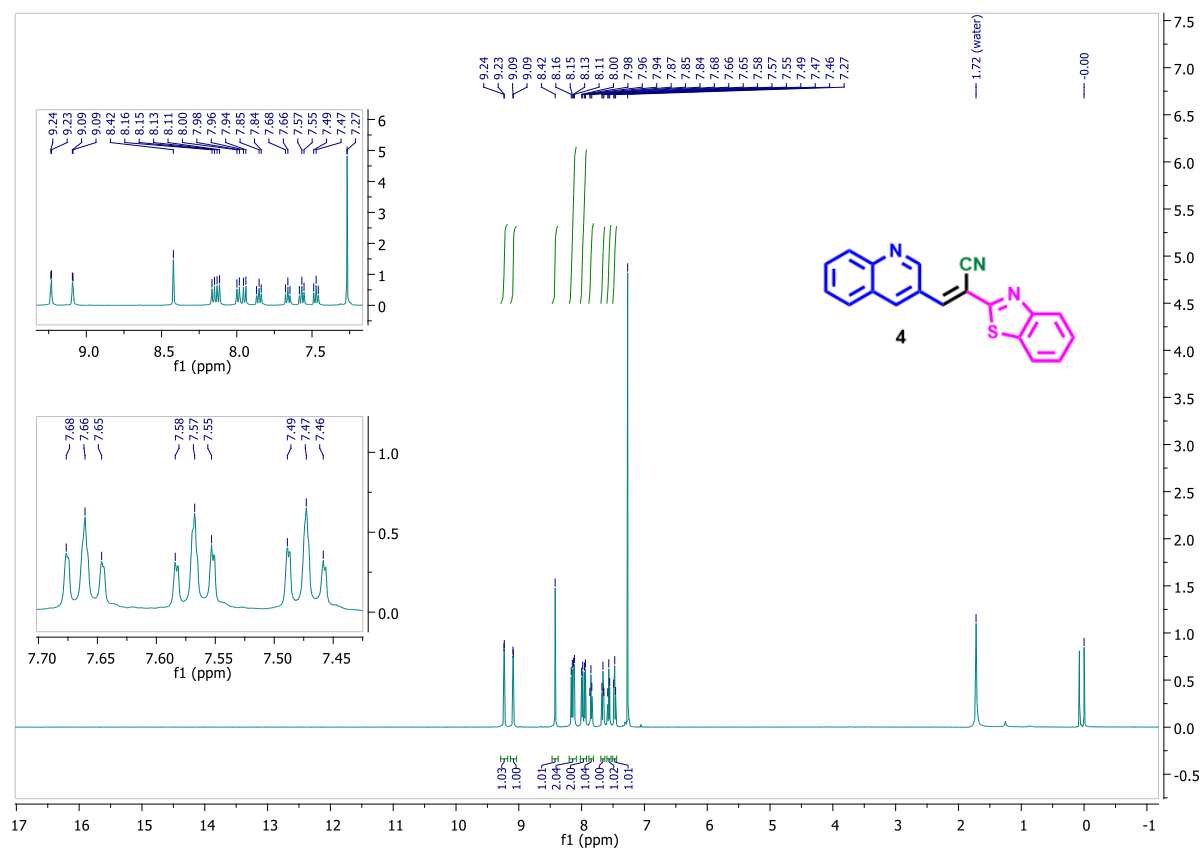
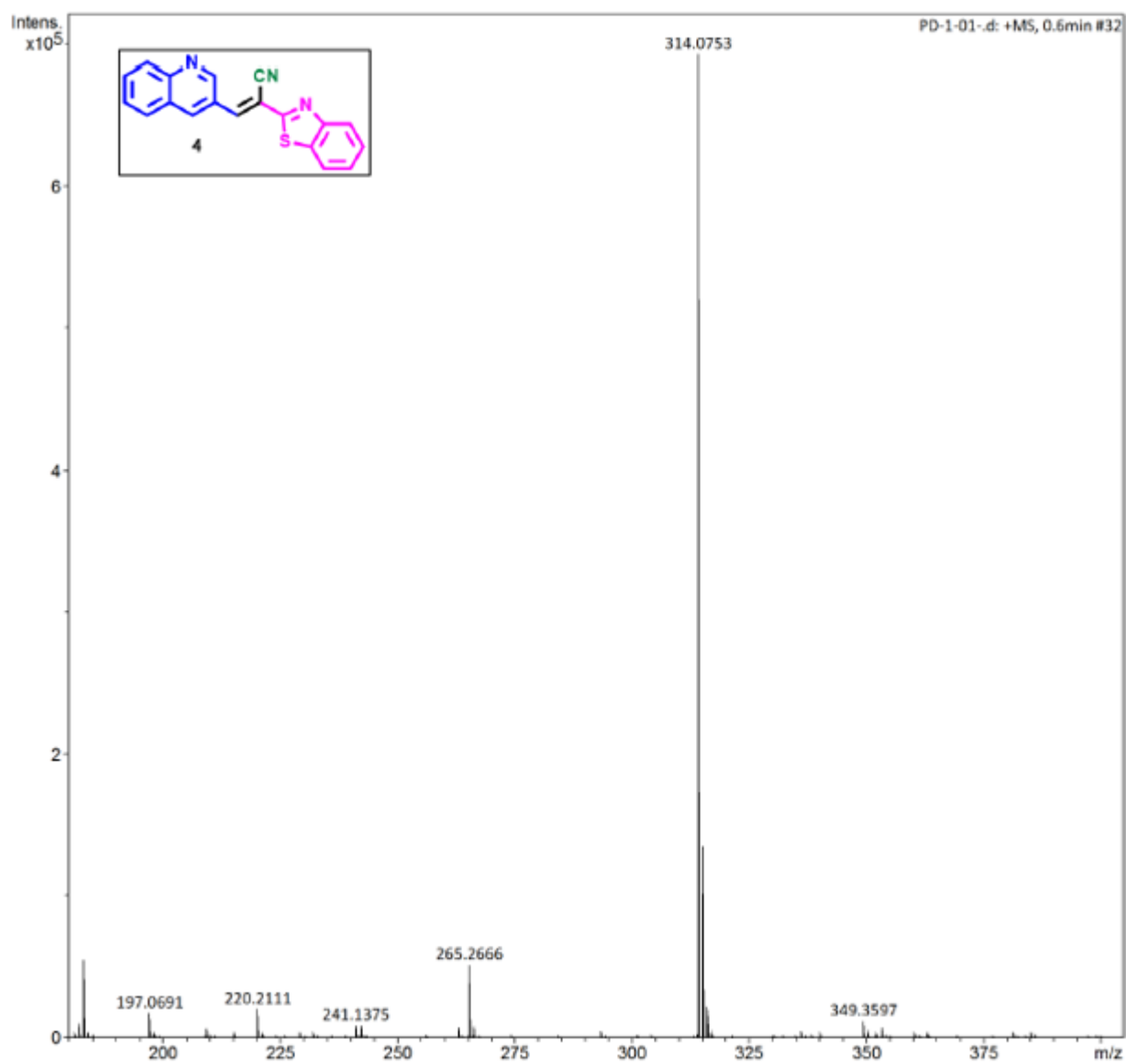


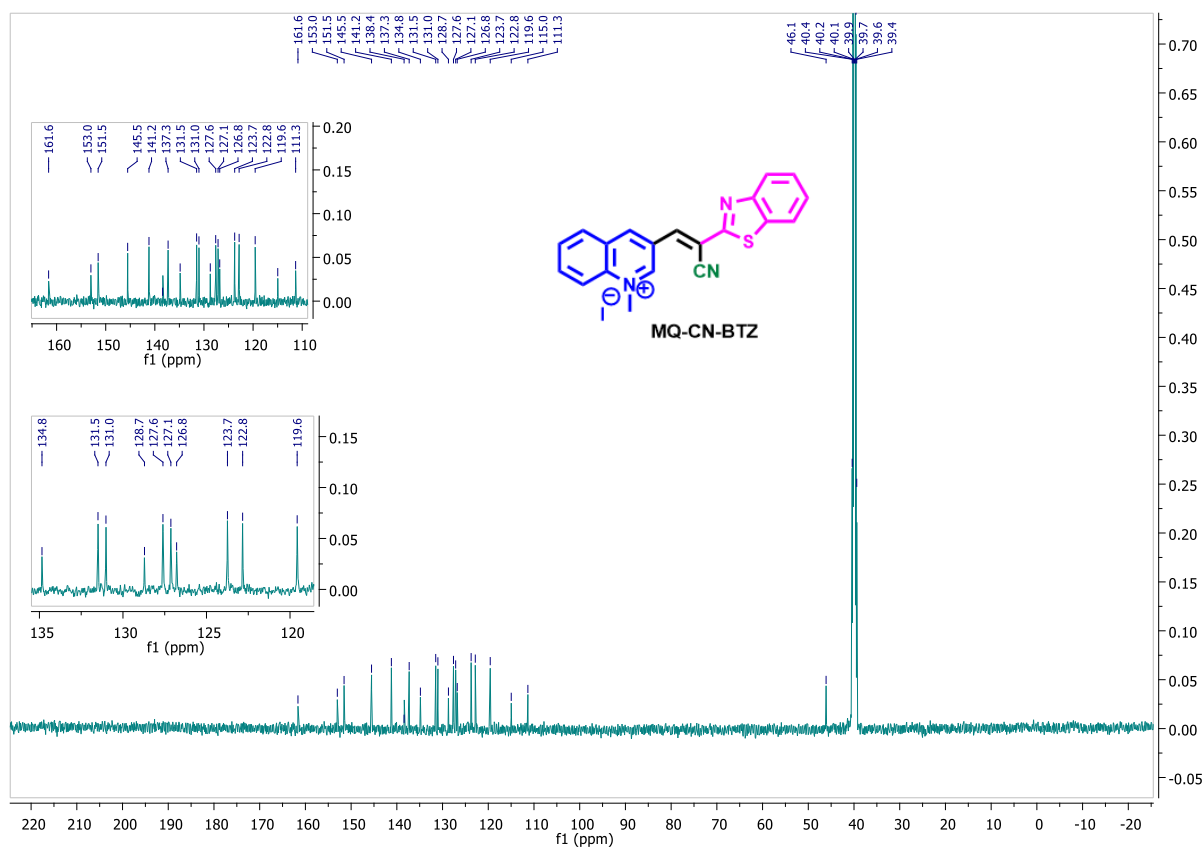
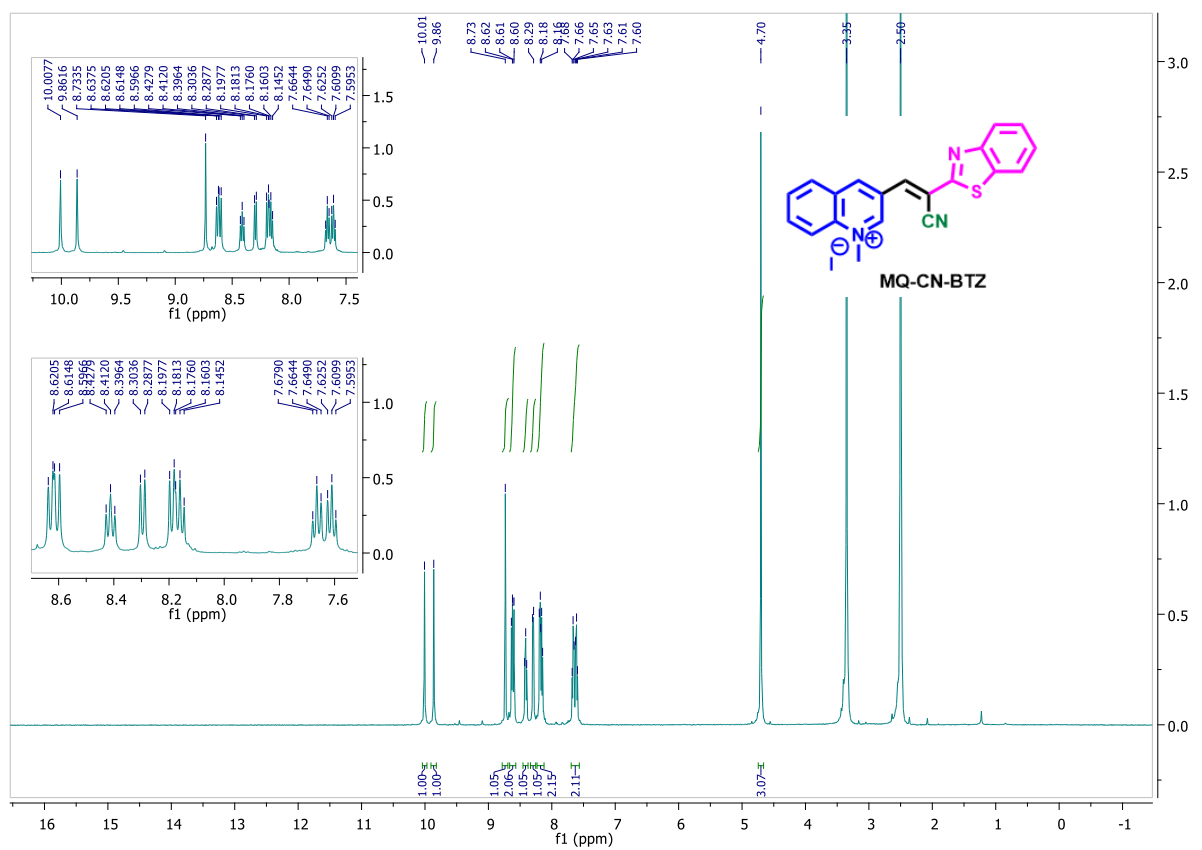
Figure S2. HRMS spectra of compound **2**



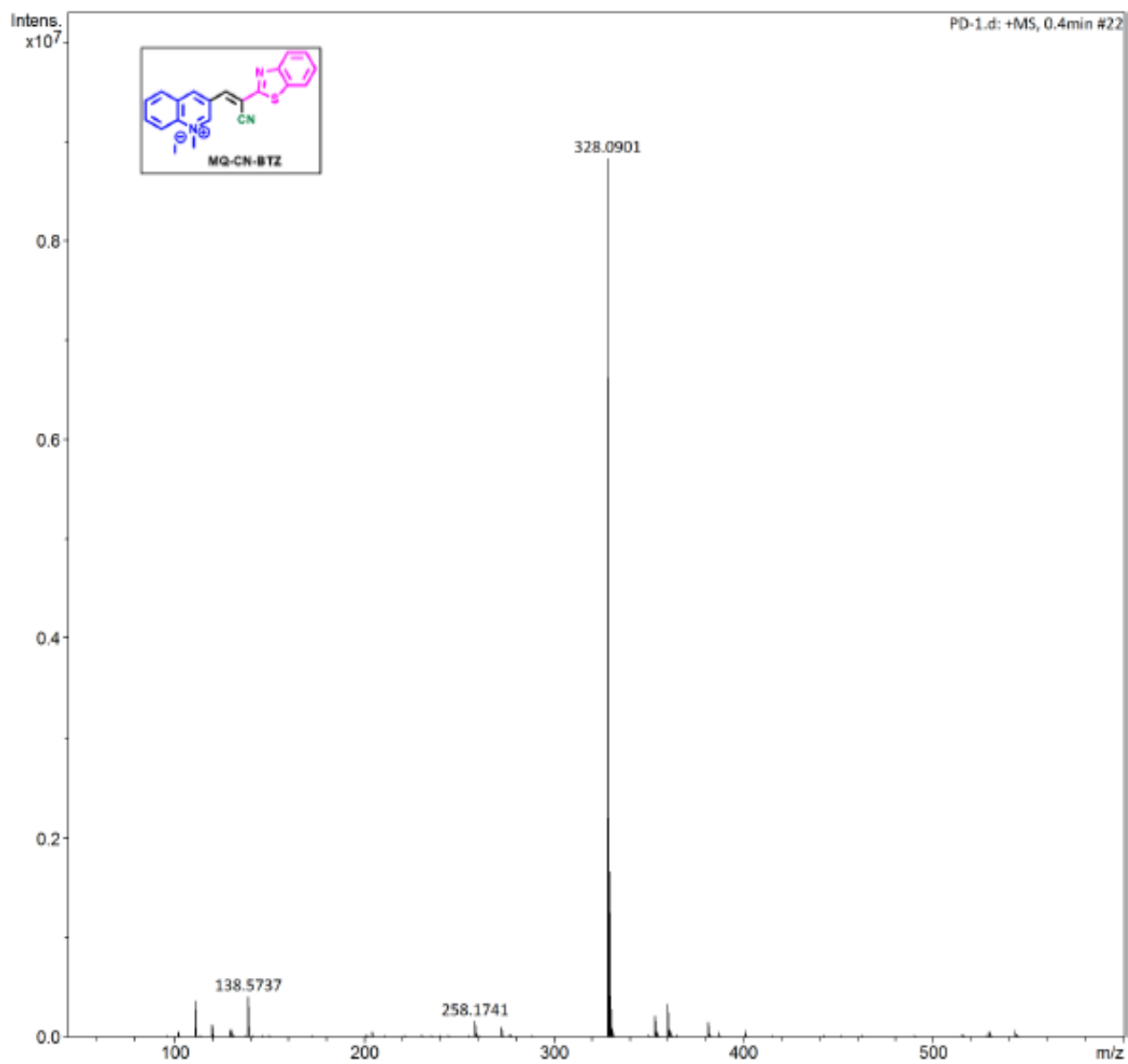
S3. ¹H and ¹³C NMR spectra of 4



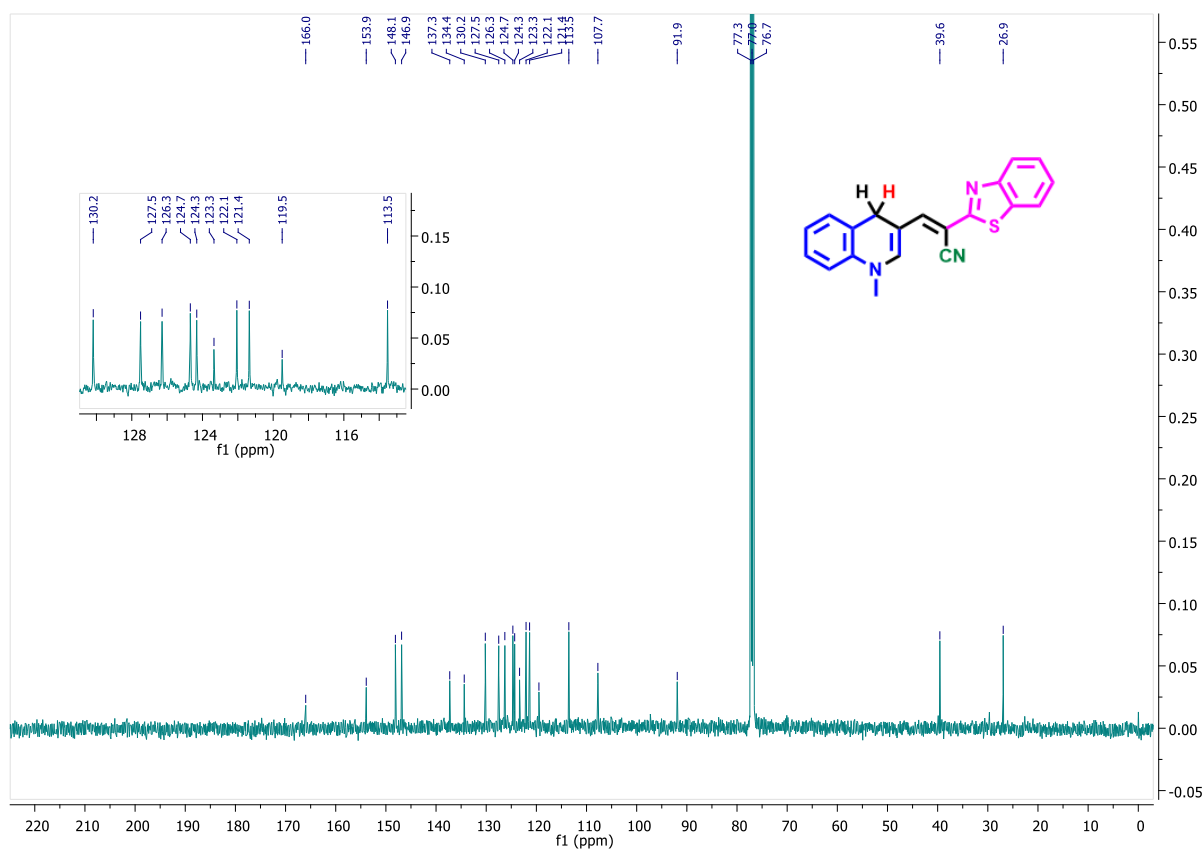
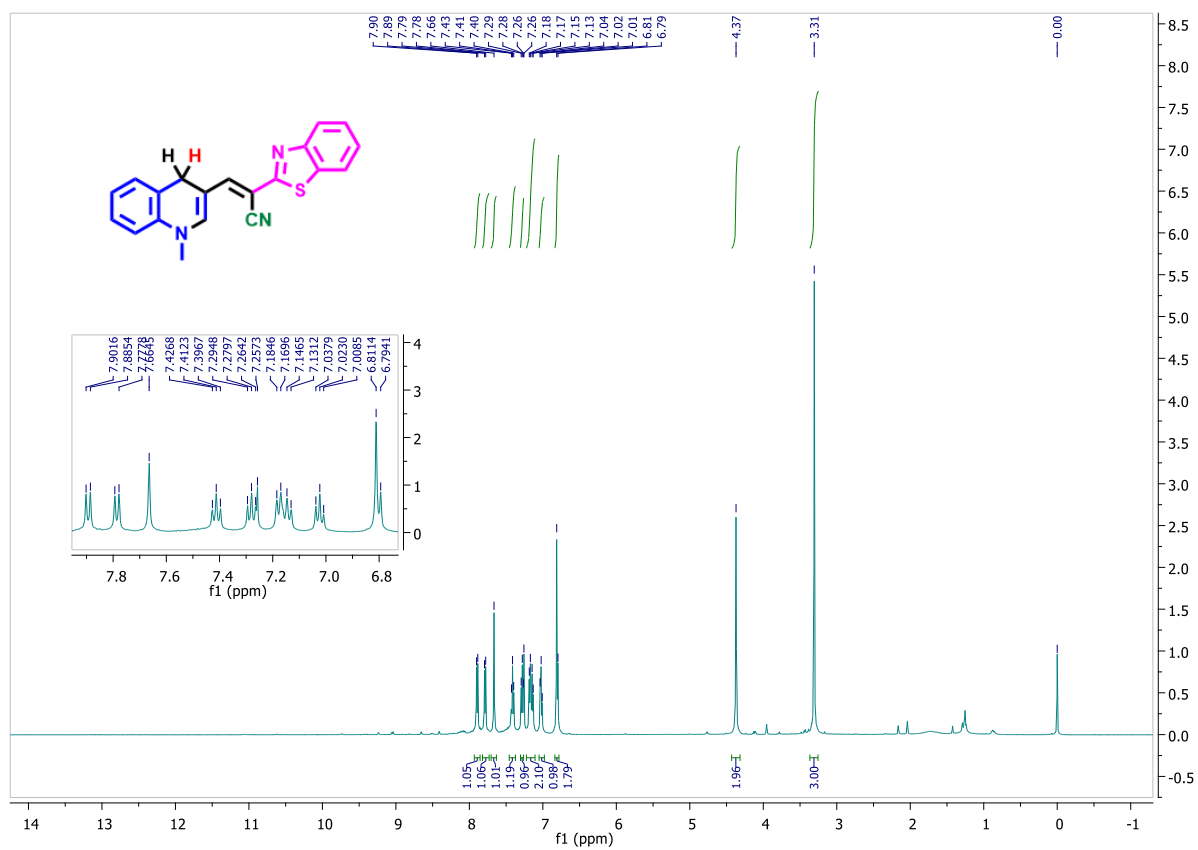
S4. HRMS spectra of compound 4.



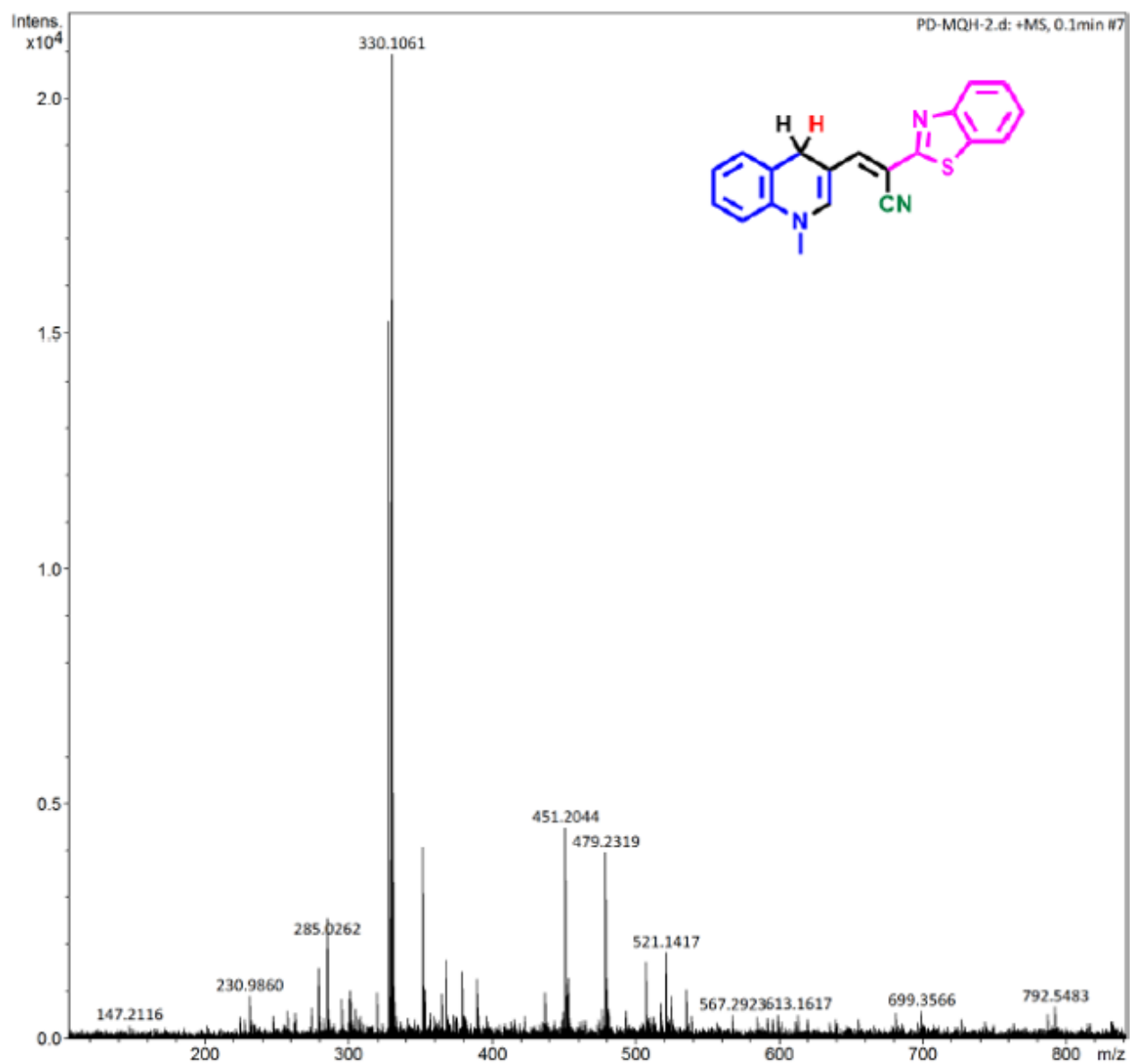
S5. ¹H and ¹³C NMR spectra of MQ-CN-BTZ.



S6. HRMS spectra of compound **MQ-CN-BTZ**.



S7. ¹H and ¹³C NMR spectra of MQ-CN-BTZH.



S8. HRMS spectra of compound **MQ-CN-BTZH**.

5. Optical behaviour of MQ-CN-BTZ

Fluorescence response of MQ-CN-BTZ (10 μ M) towards various analytes:

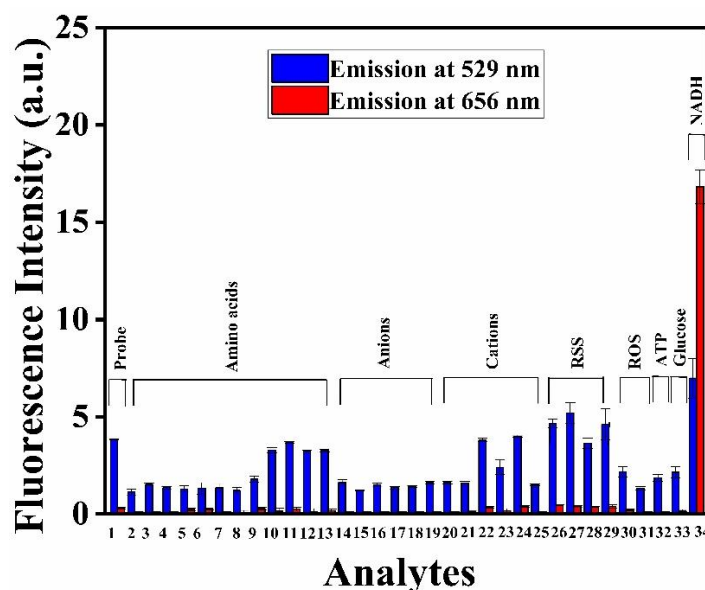


Figure S9. Fluorescence response of MQ-CN-BTZ (10 μ M) towards various analytes (300 μ M) and NADH (300 μ M) in PBS buffer (10 mM, pH \sim 7.4) after incubation at 37 $^{\circ}$ C for 15 min and recorded at two different emission wavelengths, viz \sim 529 nm and \sim 656 nm ($\lambda_{\text{ex}} = 475$ nm): (1) control, (2) glutamic acid, (3) asparagine, (4) arginine, (5) methionine, (6) glutamine, (7) tryptophan, (8) threonine, (9) valine, (10) phenylalanine, (11) aspartic acid, (12) tyrosine, (13) alanine, (14) I^- , (15) F^- , (16) Br^- , (17) Cl^- , (18) NO_3^- , (19) SO_4^{2-} , (20) Co^{2+} , (21) Zn^{2+} , (22) Na^+ , (23) Mg^{2+} , (24) Ca^{2+} , (25) K^+ , (26) cysteine, (27) NaSH, (28) glutathione, (29) homocysteine, (30) H_2O_2 , (31) NaOCl, (32) ATP, (33) glucose and (34) NADH. The blue bar represents the emission of MQ-CN-BTZ towards various analytes and NADH at \sim 529 nm, and the red bar represents the emission at \sim 656 nm ($\lambda_{\text{ex}} = 475$ nm).

Fluorescence emission profile of **MQ-CN-BTZ** with increasing concentration of NADH (10-50 μM):

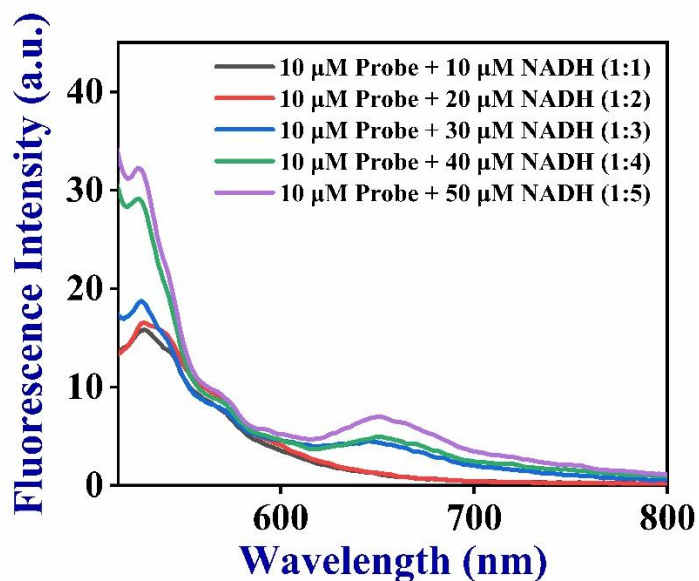


Figure S10. Fluorescence emission profile of **MQ-CN-BTZ** (10 μM) in the presence of increasing equivalents of NADH (10-50 μM).

THF-Water experiment for the probe **MQ-CN-BTZ**:

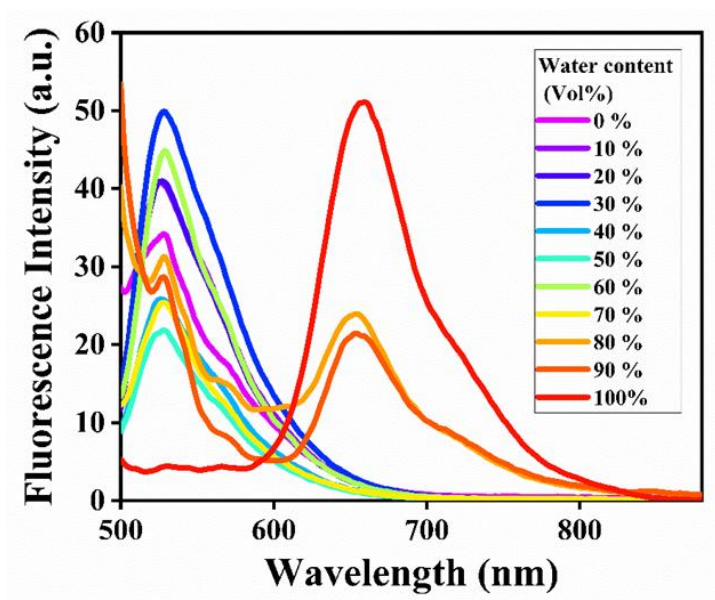


Figure S11. Fluorescence spectra of the probe (10 μM) were recorded using varied ratios of THF-water mixtures in the presence of NADH (300 μM) (Incubation time:15 mins at 37°C).

Table S1: Average lifetime of **MQ-CN-BTZ** in the presence of different equivalents of NADH at 529 nm.

Different equivalents of NADH	τ_1 (ns)	τ_2 (ns)	τ_3 (ns)	χ^2	Average lifetime (ns) at 529 nm
1 equivalent of NADH	0.631	0.047	4.80	1.00	0.055
2 equivalents of NADH	0.807	0.027	4.40	0.96	0.030
3 equivalents of NADH	0.785	0.029	4.70	0.97	0.032
10 equivalents of NADH	0.905	0.055	4.36	1.00	0.064
20 equivalents of NADH	0.781	0.026	4.57	1.07	0.028
30 equivalents of NADH	0.764	0.031	4.78	1.02	0.034

Table S2: Average lifetime of **MQ-CN-BTZ** in the presence of different equivalents of NADH at 656 nm.

Different equivalents of NADH	τ_1 (ns)	τ_2 (ns)	τ_3 (ns)	χ^2	Average lifetime (ns) at 656 nm
10 equivalents of NADH	0.207	1.07	2.83	0.96	0.44
20 equivalents of NADH	0.498	1.77	-	1.08	0.78
30 equivalents of NADH	0.481	1.77	-	1.11	0.77

6. MTT assay for MQ-CN-BTZ

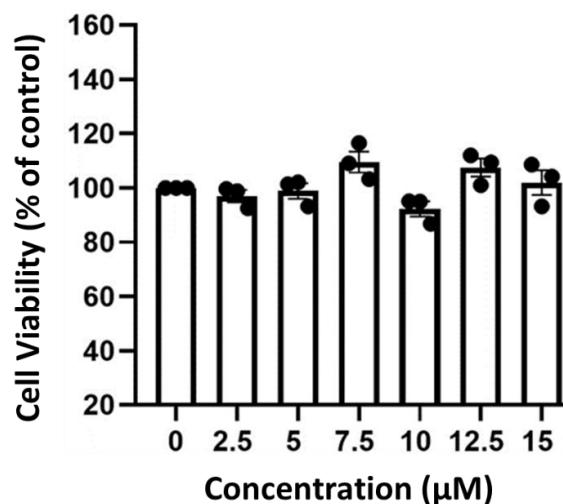
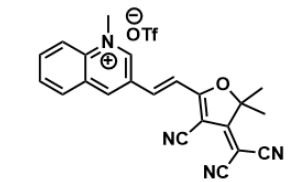
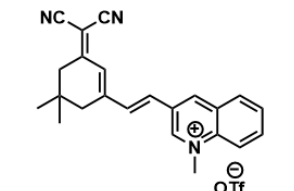
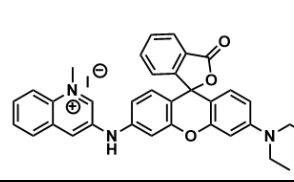
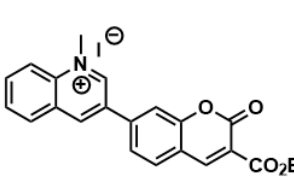
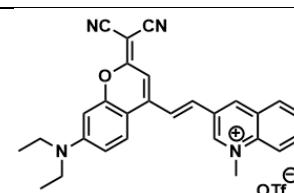
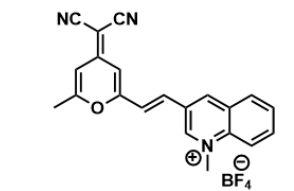
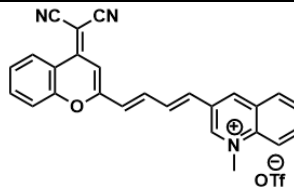
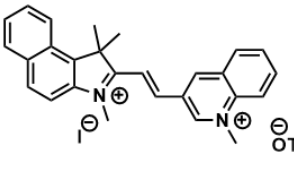
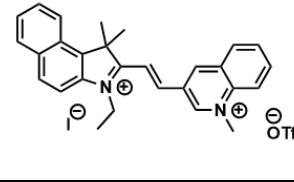
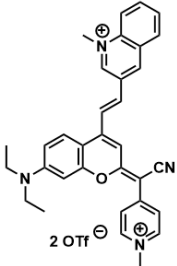
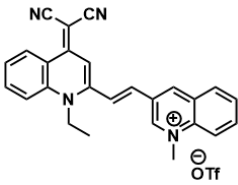
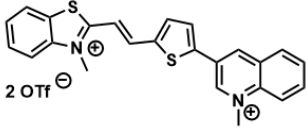
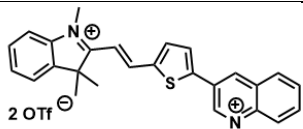
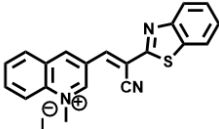


Figure S12. Cell viabilities of HepG2 cells treated with different concentrations (0–15 μM) of MQ-CN-BTZ and recorded for 24 h.

7. Table S3: Performance parameters of some of the reported efficient probes for NADH/NADPH detection and cellular imaging.

S. No.	Structure	$\lambda_{\text{ex}}/\lambda_{\text{em}}$ (nm)	Stokes shift (nm)	Fluorescence response	Response time	Application	Reference
1.		537/561	24	Turn ON	5 min	Cells and tumor spheroid model	<i>ACS Sens.</i> , 2016, 1 , 702-709. ⁵
2.		480/575	95	Turn ON	20 min	Cells	<i>J. Am. Chem. Soc.</i> , 2016, 138 , 10394-10397. ⁶
3.		560/650	90	Turn OFF	10 min	Cells	<i>Tetrahedron Lett.</i> , 2018, 59 , 3210-3213. ⁷

4.		582/610	28	Turn ON	25 min	Cells and mice	<i>Chem. Sci.</i> , 2019, 10 , 8179-8186. ⁸
5.		568/660	92	Turn ON	15 min	Cells and mice	<i>Anal. Chem.</i> , 2018, 91 , 1368-1374. ⁹
6.		525/560	35	Turn ON	2 h	Cells	<i>Chem. Commun.</i> , 2019, 55 , 537-540. ¹⁰
7.		390/460	70	Turn ON	60 min	Cells and tumor tissue	<i>Sens. Actuators, B</i> , 2020, 324 , 128637. ¹¹
8.		590/640	50	Turn ON	80 min	Cells	<i>Sens. Actuators, B</i> , 2020, 320 , 128360. ¹²
9.		510/624	114	Turn ON	60 min	Cells	<i>J. Mater. Chem. B</i> , 2021, 9 , 9547-9552. ¹³
10.		595/670	75	Turn ON	20 min	Cells	<i>Sens. Actuators, B</i> , 2022, 350 , 130862. ¹⁴
11.		475/580	105	Turn ON	10 min	Cells and mice	<i>Talanta</i> , 2023, 257 , 124393. ¹⁵
12.		520/584	64	Turn ON	4 min	Cells and tumor spheroids	<i>ACS Sens.</i> , 2023, 8 , 829-838. ¹⁶

13.		600/670	70	Turn ON	60 min	Cells and fruit fly larvae	<i>ACS Appl. Bio Mater.</i> , 2024, 7 , 8465-8478. ¹⁷
14.		543/620	77	Turn ON	30 min	Cells and mice	<i>Sens. Actuators, B</i> , 2024, 409 , 135618. ¹⁸
15.		630/748	118	Turn ON	60 min	Cells and larvae of <i>D. melanogaster</i>	<i>J. Mater: Chem. B</i> , 2024, 12 , 448-465. ¹⁹
16.		680/ 742.1	62.1	Turn ON	75 min	Cells and fruit fly larvae	<i>Sens. Actuators, B</i> , 2024, 402 , 135073. ²⁰
17.		475/529, 656	54, 181	Turn ON	15 min	Cells	This work

8. References

1. B. Vidya, M. Iniya, G. Sivaraman and R. V. Sumesh, Diverse benzothiazole based chemodosimeters for the detection of cyanide in aqueous media and in HeLa cells, *Sens. Actuators, B*, 2017, **242**, 434-442.
2. S. S. AlNeyadi, A. A. Salem, M. A. Ghattas, N. Atatreh and I. M. Abdou, Antibacterial activity and mechanism of action of the benzazole acrylonitrile-based compounds: In vitro, spectroscopic, and docking studies, *Eur. J. Med. Chem*, 2017, **136**, 270-282.
3. H. S. Elzahabi, Synthesis, characterization of some benzazoles bearing pyridine moiety: Search for novel anticancer agents, *Eur. J. Med. Chem*, 2011, **46**, 4025-4034.

4. K. Wang, G. Lai, Z. Li, M. Liu, Y. Shen and C. Wang, A novel colorimetric and fluorescent probe for the highly selective and sensitive detection of palladium based on Pd(0) mediated reaction, *Tetrahedron*, 2015, **71**, 7874-7878.
5. M. A. Fomin, R. I. Dmitriev, J. Jenkins, D. B. Papkovsky, D. Heindl and B. König, Two-Acceptor Cyanine-Based Fluorescent Indicator for NAD(P)H in Tumor Cell Models, *ACS Sens.*, 2016, **1**, 702-709.
6. L. Wang, J. Zhang, B. Kim, J. Peng, S. N. Berry, Y. Ni, D. Su, J. Lee, L. Yuan and Y.-T. Chang, Boronic Acid: A Bio-Inspired Strategy To Increase the Sensitivity and Selectivity of Fluorescent NADH Probe, *J. Am. Chem. Soc.*, 2016, **138**, 10394-10397.
7. M. Santra, S. Sarkar, Y. W. Jun, Y. J. Reo and K. H. Ahn, Dual probing of redox species, NAD(P)H and HOCl, with a benzo[a]phenoxazine based far red-emitting dye, *Tetrahedron Lett.*, 2018, **59**, 3210-3213.
8. X. Pan, Y. Zhao, T. Cheng, A. Zheng, A. Ge, L. Zang, K. Xu and B. Tang, Monitoring NAD(P)H by an ultrasensitive fluorescent probe to reveal reductive stress induced by natural antioxidants in HepG2 cells under hypoxia, *Chem. Sci.*, 2019, **10**, 8179-8186.
9. Y. Zhao, K. Wei, F. Kong, X. Gao, K. Xu and B. Tang, Dicyanoisophorone-Based Near-Infrared Emission Fluorescent Probe for Detecting NAD(P)H in Living Cells and in Vivo, *Anal. Chem.*, 2018, **91**, 1368-1374.
10. J. SeungáKim, A rhodamine based fluorescent probe validates substrate and cellular hypoxia specific NADH expression, *Chem. Commun.*, 2019, **55**, 537-540.
11. A. Podder, N. Thirumalaivasan, Y. K. Chao, P. Kukutla, S.-P. Wu and S. Bhuniya, Two-photon active fluorescent indicator for detecting NADH dynamics in live cells and tumor tissue, *Sens. Actuators, B*, 2020, **324**, 128637.
12. J. H. Joo, M. Won, S. Y. Park, K. Park, D.-S. Shin, J. S. Kim and M. H. Lee, A dicyanocoumarin-fused quinolinium based probe for NAD(P)H and its use for detecting glycolysis and hypoxia in living cells and tumor spheroids, *Sens. Actuators, B*, 2020, **320**, 128360.
13. M. Li, C. Liu, W. Zhang, L. Xu, M. Yang, Z. Chen, X. Wang, L. Pu, W. Liu and X. Zeng, An NADH-selective and sensitive fluorescence probe to evaluate living cell hypoxic stress, *J. Mater. Chem. B*, 2021, **9**, 9547-9552.

14. H. Wei, Y. Yu, G. Wu, Y. Wang, S. Duan, J. Han, W. Cheng, C. Li, X. Tian and X. Zhang, Dual-responsive fluorescent probe for imaging NAD(P)H and mitochondrial viscosity and its application in cancer cell ferroptosis, *Sens. Actuators, B*, 2022, **350**, 130862.
15. Q. Wang, Y. Zhu, D. Chen, J. Ou, M. Chen, Y. Feng, W. Wang and X. Meng, A dual-salt fluorescent probe for specific recognition of mitochondrial NADH and potential cancer diagnosis, *Talanta*, 2023, **257**, 124393.
16. H. Chang, X. Hu, X. Tang, S. Tian, Y. Li, X. Lv and L. Shang, A Mitochondria-Targeted Fluorescent Probe for Monitoring NADPH Overproduction during Influenza Virus Infection, *ACS Sens.*, 2023, **8**, 829-838.
17. S. Jaeger, H. Lanquaye, S. K. Dwivedi, D. L. Arachchige, J. Xia, M. Waters, B. L. Bigari, A. M. Olowolagba, P. Agyemang and Y. Zhang, Near-Infrared Visualization of NAD(P)H Dynamics in Live Cells and *Drosophila melanogaster* Larvae Using a Coumarin-Based Pyridinium Fluorescent Probe, *ACS Appl. Bio Mater.*, 2024, **7**, 8465-8478.
18. Y. Cao, L. Yuan, W. Liu, Y. Ye, Q. Jiao, H.-l. Zhu and Z. Wang, Detection of NAD(P)H by fluorescent probe to reveal the protective effects of natural antioxidants on acute liver injury, *Sens. Actuators, B*, 2024, **409**, 135618.
19. D. L. Arachchige, S. K. Dwivedi, M. Waters, S. Jaeger, J. Peters, D. R. Tucker, M. Geborkoff, T. Werner, R. L. Luck and B. Godugu, Sensitive monitoring of NAD(P)H levels within cancer cells using mitochondria-targeted near-infrared cyanine dyes with optimized electron-withdrawing acceptors, *J. Mater: Chem. B*, 2024, **12**, 448-465.
20. S. K. Dwivedi, D. L. Arachchige, M. Waters, S. Jaeger, M. Mahmoud, A. M. Olowolagba, D. R. Tucker, M. R. Geborkoff, T. Werner and R. L. Luck, Near-infrared absorption and emission probes with optimal connection bridges for live monitoring of NAD(P)H dynamics in living systems, *Sens. Actuators, B*, 2024, **402**, 135073.